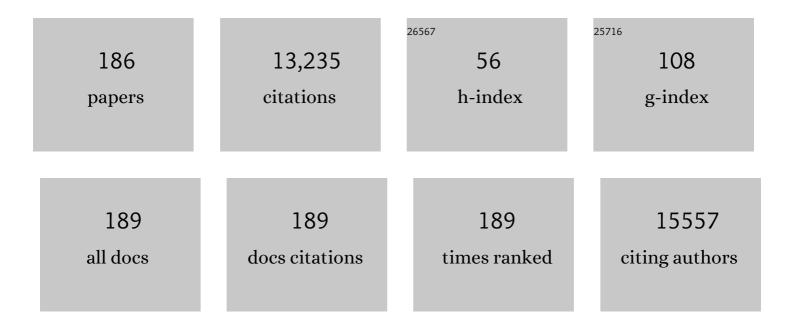
Qinghong Zhang

List of Publications by Year in descending order

Source: https://exaly.com/author-pdf/4489775/publications.pdf Version: 2024-02-01



ΟΙΝCHONC ΖΗΛΝΟ

#	Article	IF	CITATIONS
1	Design and Mechanisms of Asymmetric Supercapacitors. Chemical Reviews, 2018, 118, 9233-9280.	23.0	2,379
2	Graphene-based materials for flexible supercapacitors. Chemical Society Reviews, 2015, 44, 3639-3665.	18.7	1,015
3	3D Freezeâ€Casting of Cellular Graphene Films for Ultrahighâ€Powerâ€Density Supercapacitors. Advanced Materials, 2016, 28, 6719-6726.	11.1	390
4	All-fiber hybrid piezoelectric-enhanced triboelectric nanogenerator for wearable gesture monitoring. Nano Energy, 2018, 48, 152-160.	8.2	343
5	Origami-inspired active graphene-based paper for programmable instant self-folding walking devices. Science Advances, 2015, 1, e1500533.	4.7	312
6	Highly Conductive, Flexible, and Compressible Allâ€Graphene Passive Electronic Skin for Sensing Human Touch. Advanced Materials, 2014, 26, 5018-5024.	11.1	273
7	Flexible quasi-solid-state planar micro-supercapacitor based on cellular graphene films. Materials Horizons, 2017, 4, 1145-1150.	6.4	222
8	Sheath-run artificial muscles. Science, 2019, 365, 150-155.	6.0	218
9	Earth-Abundant Oxygen Electrocatalysts for Alkaline Anion-Exchange-Membrane Water Electrolysis: Effects of Catalyst Conductivity and Comparison with Performance in Three-Electrode Cells. ACS Catalysis, 2019, 9, 7-15.	5.5	189
10	Ultrathin, Washable, and Largeâ€Area Graphene Papers for Personal Thermal Management. Small, 2017, 13, 1702645.	5.2	177
11	Advanced Functional Fiber and Smart Textile. Advanced Fiber Materials, 2019, 1, 3-31.	7.9	169
12	Molecular-channel driven actuator with considerations for multiple configurations and color switching. Nature Communications, 2018, 9, 590.	5.8	159
13	High-performance flexible asymmetric supercapacitors based on 3D porous graphene/MnO ₂ nanorod and graphene/Ag hybrid thin-film electrodes. Journal of Materials Chemistry C, 2013, 1, 1245-1251.	2.7	156
14	An Elastic Transparent Conductor Based on Hierarchically Wrinkled Reduced Graphene Oxide for Artificial Muscles and Sensors. Advanced Materials, 2016, 28, 9491-9497.	11.1	147
15	Flexible and high-performance electrochromic devices enabled by self-assembled 2D TiO2/MXene heterostructures. Nature Communications, 2021, 12, 1587.	5.8	143
16	Morphology-tailored synthesis of vertically aligned 1D WO ₃ nano-structure films for highly enhanced electrochromic performance. Journal of Materials Chemistry A, 2013, 1, 684-691.	5.2	140
17	Anatase TiO2 nanoparticles immobilized on ZnO tetrapods as a highly efficient and easily recyclable photocatalyst. Applied Catalysis B: Environmental, 2007, 76, 168-173.	10.8	137
18	lon-Transport Design for High-Performance Na ⁺ -Based Electrochromics. ACS Nano, 2018, 12, 3759-3768.	7.3	136

#	Article	IF	CITATIONS
19	Fluoroalkylsilane-Modified Textile-Based Personal Energy Management Device for Multifunctional Wearable Applications. ACS Applied Materials & Interfaces, 2016, 8, 4676-4683.	4.0	130
20	Enhanced Power Output of a Triboelectric Nanogenerator Composed of Electrospun Nanofiber Mats Doped with Graphene Oxide. Scientific Reports, 2015, 5, 13942.	1.6	123
21	Continuous and scalable manufacture of amphibious energy yarns and textiles. Nature Communications, 2019, 10, 868.	5.8	121
22	All-fiber tribo-ferroelectric synergistic electronics with high thermal-moisture stability and comfortability. Nature Communications, 2019, 10, 5541.	5.8	121
23	A highly integrated sensing paper for wearable electrochemical sweat analysis. Biosensors and Bioelectronics, 2021, 174, 112828.	5.3	113
24	MXene-Coated Air-Permeable Pressure-Sensing Fabric for Smart Wear. ACS Applied Materials & Interfaces, 2020, 12, 46446-46454.	4.0	111
25	Ta3N5Nanoparticles with Enhanced Photocatalytic Efficiency under Visible Light Irradiation. Langmuir, 2004, 20, 9821-9827.	1.6	110
26	Aluminumâ€lonâ€Intercalation Supercapacitors with Ultrahigh Areal Capacitance and Highly Enhanced Cycling Stability: Power Supply for Flexible Electrochromic Devices. Small, 2017, 13, 1700380.	5.2	107
27	High-performance all-solid-state yarn supercapacitors based on porous graphene ribbons. Nano Energy, 2015, 12, 26-32.	8.2	101
28	Cladding nanostructured AgNWs-MoS2 electrode material for high-rate and long-life transparent in-plane micro-supercapacitor. Energy Storage Materials, 2019, 16, 212-219.	9.5	99
29	Hierarchical NiO microflake films with high coloration efficiency, cyclic stability and low power consumption for applications in a complementary electrochromic device. Nanoscale, 2013, 5, 4808.	2.8	97
30	Red, Green, Blue (RGB) Electrochromic Fibers for the New Smart Color Change Fabrics. ACS Applied Materials & Interfaces, 2014, 6, 13043-13050.	4.0	97
31	Highâ€Performance Flexible Thermoelectric Devices Based on Allâ€Inorganic Hybrid Films for Harvesting Lowâ€Grade Heat. Advanced Functional Materials, 2019, 29, 1900304.	7.8	97
32	Fluorinated metal-organic framework as bifunctional filler toward highly improving output performance of triboelectric nanogenerators. Nano Energy, 2020, 70, 104517.	8.2	97
33	A Moisture-Wicking Passive Radiative Cooling Hierarchical Metafabric. ACS Nano, 2022, 16, 2188-2197.	7.3	96
34	A multi-responsive water-driven actuator with instant and powerful performance for versatile applications. Scientific Reports, 2015, 5, 9503.	1.6	91
35	Synergistic Solvation and Interface Regulations of Ecoâ€Friendly Silk Peptide Additive Enabling Stable Aqueous Zincâ€Ion Batteries. Advanced Functional Materials, 2022, 32, .	7.8	91
36	Regulation of carbon content in MOF-derived hierarchical-porous NiO@C films for high-performance electrochromism. Materials Horizons, 2019, 6, 571-579.	6.4	90

#	Article	IF	CITATIONS
37	Hierarchical nanostructure of WO3 nanorods on TiO2 nanofibers and the enhanced visible light photocatalytic activity for degradation of organic pollutants. CrystEngComm, 2013, 15, 5986.	1.3	88
38	S, N Co-Doped Graphene Quantum Dot/TiO2 Composites for Efficient Photocatalytic Hydrogen Generation. Nanoscale Research Letters, 2017, 12, 400.	3.1	87
39	Stable Hydrogel Electrolytes for Flexible and Submarine-Use Zn-Ion Batteries. ACS Applied Materials & Interfaces, 2020, 12, 46005-46014.	4.0	87
40	Preparation and magnetic property analysis of monodisperse Co–Zn ferrite nanospheres. Journal of Alloys and Compounds, 2010, 491, 431-435.	2.8	83
41	Infrared-Radiation-Enhanced Nanofiber Membrane for Sky Radiative Cooling of the Human Body. ACS Applied Materials & Interfaces, 2019, 11, 44673-44681.	4.0	82
42	Graphene–polymer hydrogels with stimulus-sensitive volume changes. Carbon, 2012, 50, 1959-1965.	5.4	81
43	Lattice-contraction triggered synchronous electrochromic actuator. Nature Communications, 2018, 9, 4798.	5.8	80
44	Facilitating Interfacial Stability Via Bilayer Heterostructure Solid Electrolyte Toward Highâ€energy, Safe and Adaptable Lithium Batteries. Advanced Energy Materials, 2020, 10, 2000709.	10.2	79
45	Bio-applicable and electroactive near-infrared laser-triggered self-healing hydrogels based on graphene networks. Journal of Materials Chemistry, 2012, 22, 14991.	6.7	76
46	A wearable, fibroid, self-powered active kinematic sensor based on stretchable sheath-core structural triboelectric fibers. Nano Energy, 2017, 39, 673-683.	8.2	71
47	Self-seeded growth of nest-like hydrated tungsten trioxide film directly on FTO substrate for highly enhanced electrochromic performance. Journal of Materials Chemistry A, 2014, 2, 11305-11310.	5.2	70
48	Abrasion Resistant/Waterproof Stretchable Triboelectric Yarns Based on Fermat Spirals. Advanced Materials, 2021, 33, e2100782.	11.1	68
49	Facile growth of vertically aligned BiOCl nanosheet arrays on conductive glass substrate with high photocatalytic properties. Journal of Materials Chemistry, 2012, 22, 16851.	6.7	67
50	ZnO Nanoparticles Immobilized on Flaky Layered Double Hydroxides as Photocatalysts with Enhanced Adsorptivity for Removal of Acid Red G. Langmuir, 2010, 26, 15546-15553.	1.6	65
51	Self-weaving WO3 nanoflake films with greatly enhanced electrochromic performance. Journal of Materials Chemistry, 2012, 22, 16633.	6.7	65
52	A high efficiency microreactor with Pt/ZnO nanorod arrays on the inner wall for photodegradation of phenol. Journal of Hazardous Materials, 2013, 254-255, 318-324.	6.5	65
53	Modifying Perovskite Films with Polyvinylpyrrolidone for Ambient-Air-Stable Highly Bendable Solar Cells. ACS Applied Materials & Interfaces, 2018, 10, 35385-35394.	4.0	64
54	Spray coated ultrathin films from aqueous tungsten molybdenum oxide nanoparticle ink for high contrast electrochromic applications. Journal of Materials Chemistry C, 2016, 4, 33-38.	2.7	63

#	Article	IF	CITATIONS
55	Investigation on the physical–mechanical properties of dental resin composites reinforced with novel bimodal silica nanostructures. Materials Science and Engineering C, 2015, 50, 266-273.	3.8	60
56	Spray-coated monodispersed SnO2 microsphere films as scaffold layers for efficient mesoscopic perovskite solar cells. Journal of Power Sources, 2020, 448, 227405.	4.0	58
57	Selfâ€Powered Interactive Fiber Electronics with Visual–Digital Synergies. Advanced Materials, 2021, 33, e2104681.	11.1	58
58	Wearable Thermoelectric Devices Based on Au-Decorated Two-Dimensional MoS ₂ . ACS Applied Materials & Interfaces, 2018, 10, 33316-33321.	4.0	57
59	Controllable growth of high-quality metal oxide/conducting polymer hierarchical nanoarrays with outstanding electrochromic properties and solar-heat shielding ability. Journal of Materials Chemistry A, 2014, 2, 13541-13549.	5.2	56
60	Facile fabrication of a magnetically induced structurally colored fiber and its strain-responsive properties. Journal of Materials Chemistry A, 2015, 3, 11093-11097.	5.2	54
61	Highly Integrable Thermoelectric Fiber. ACS Applied Materials & amp; Interfaces, 2020, 12, 33297-33304.	4.0	54
62	Highly Strong and Elastic Graphene Fibres Prepared from Universal Graphene Oxide Precursors. Scientific Reports, 2014, 4, 4248.	1.6	53
63	Wicking–Polarizationâ€Induced Water Cluster Size Effect on Triboelectric Evaporation Textiles. Advanced Materials, 2021, 33, e2007352.	11.1	53
64	Low shrinkage light curable dental nanocomposites using SiO2 microspheres as fillers. Materials Science and Engineering C, 2012, 32, 2115-2121.	3.8	52
65	Dual-Mechanism and Multimotion Soft Actuators Based on Commercial Plastic Film. ACS Applied Materials & amp; Interfaces, 2018, 10, 15122-15128.	4.0	52
66	Water-resistant and underwater adhesive ion-conducting gel for motion-robust bioelectric monitoring. Chemical Engineering Journal, 2022, 431, 134012.	6.6	52
67	Aqueous synthesis of high bright and tunable near-infrared AgInSe 2 –ZnSe quantum dots for bioimaging. Journal of Colloid and Interface Science, 2016, 463, 1-7.	5.0	49
68	Solutionâ€Processed Porous Tungsten Molybdenum Oxide Electrodes for Energy Storage Smart Windows. Advanced Materials Technologies, 2017, 2, 1700047.	3.0	48
69	Grain engineering by ultrasonic substrate vibration post-treatment of wet perovskite films for annealing-free, high performance, and stable perovskite solar cells. Nanoscale, 2018, 10, 8526-8535.	2.8	48
70	Continuously Processed, Long Electrochromic Fibers with Multi-Environmental Stability. ACS Applied Materials & Interfaces, 2020, 12, 28451-28460.	4.0	48
71	Fabrication of large-area and high-crystallinity photoreduced graphene oxide films via reconstructed two-dimensional multilayer structures. NPG Asia Materials, 2014, 6, e119-e119.	3.8	47
72	Flexible and thermostable thermoelectric devices based on large-area and porous all-graphene films. Carbon, 2016, 107, 146-153.	5.4	47

#	Article	IF	CITATIONS
73	Hydrophobic coating over a CH ₃ NH ₃ PbI ₃ absorbing layer towards air stable perovskite solar cells. Journal of Materials Chemistry C, 2016, 4, 6848-6854.	2.7	47
74	Prepolymerization-assisted fabrication of an ultrathin immobilized layer to realize a semi-embedded wrinkled AgNW network for a smart electrothermal chromatic display and actuator. Journal of Materials Chemistry C, 2017, 5, 9778-9785.	2.7	46
75	Self-powered multifunctional UV and IR photodetector as an artificial electronic eye. Journal of Materials Chemistry C, 2017, 5, 1436-1442.	2.7	45
76	1T-Molybdenum disulfide/reduced graphene oxide hybrid fibers as high strength fibrous electrodes for wearable energy storage. Journal of Materials Chemistry A, 2019, 7, 3143-3149.	5.2	45
77	A remote controllable fiber-type near-infrared light-responsive actuator. Chemical Communications, 2017, 53, 11118-11121.	2.2	43
78	SnO2 nanorod arrays with tailored area density as efficient electron transport layers for perovskite solar cells. Journal of Power Sources, 2018, 402, 460-467.	4.0	42
79	ZnO nanorods decorated calcined Mg–Al layered double hydroxides as photocatalysts with a high adsorptive capacity. Colloids and Surfaces A: Physicochemical and Engineering Aspects, 2009, 348, 76-81.	2.3	41
80	Reduced graphene oxide functionalized stretchable and multicolor electrothermal chromatic fibers. Journal of Materials Chemistry C, 2017, 5, 11448-11453.	2.7	41
81	Synthesis and characterization of La2O3/TiO2â^'xFx and the visible light photocatalytic oxidation of 4-chlorophenol. Journal of Hazardous Materials, 2010, 178, 440-449.	6.5	40
82	Tuning the reactivity of PbI2 film via monolayer Ti3C2Tx MXene for two-step-processed CH3NH3PbI3 solar cells. Chemical Engineering Journal, 2021, 417, 127912.	6.6	40
83	Thermochromic Hydrogel-Functionalized Textiles for Synchronous Visual Monitoring of On-Demand <i>In Vitro</i> Drug Release. ACS Applied Materials & Interfaces, 2020, 12, 51225-51235.	4.0	39
84	Synthesis of Fe _{3} O _{4} /C/TiO _{2} Magnetic Photocatalyst via Vapor Phase Hydrolysis. International Journal of Photoenergy, 2012, 2012, 1-8.	1.4	38
85	1-Ethyl-3-methylimidazolium tetrafluoroborate-doped high ionic conductivity gel electrolytes with reduced anodic reaction potentials for electrochromic devices. Materials and Design, 2017, 118, 279-285.	3.3	38
86	High-performance solar cells with induced crystallization of perovskite by an evenly distributed CdSe quantum dots seed-mediated underlayer. Journal of Power Sources, 2018, 376, 46-54.	4.0	38
87	High performance stretchable fibrous supercapacitors and flexible strain sensors based on CNTs/MXene-TPU hybrid fibers. Electrochimica Acta, 2021, 395, 139141.	2.6	38
88	In Situ Functionalization of Stable 3D Nest‣ike Networks in Confined Channels for Microfluidic Enrichment and Detection. Advanced Functional Materials, 2014, 24, 1017-1026.	7.8	37
89	Redispersible and water-soluble LaF3:Ce,Tb nanocrystals via a microfluidic reactor with temperature steps. Journal of Materials Chemistry, 2008, 18, 5060.	6.7	36
90	A novel efficient ZnO/Zn(OH)F nanofiber arrays-based versatile microfluidic system for the applications of photocatalysis and histidine-rich protein separation. Sensors and Actuators B: Chemical, 2016, 229, 281-287.	4.0	35

#	Article	IF	CITATIONS
91	Lightweight, highly bendable and foldable electrochromic films based on all-solution-processed bilayer nanowire networks. Journal of Materials Chemistry C, 2016, 4, 5849-5857.	2.7	34
92	A single-walled carbon nanotubes/poly(3,4-ethylenedioxythiophene)-poly(styrenesulfonate)/copper hexacyanoferrate hybrid film for high-volumetric performance flexible supercapacitors. Journal of Power Sources, 2018, 386, 96-105.	4.0	34
93	Construction of hydrated tungsten trioxide nanosheet films for efficient electrochromic performance. RSC Advances, 2015, 5, 196-201.	1.7	33
94	Highâ€Performance Ionic Thermoelectric Supercapacitor for Integrated Energy Conversionâ€Storage. Energy and Environmental Materials, 2022, 5, 954-961.	7.3	33
95	Transparent Metal–Organic Framework-Based Gel Electrolytes for Generalized Assembly of Quasi-Solid-State Electrochromic Devices. ACS Applied Materials & Interfaces, 2020, 12, 42955-42961.	4.0	32
96	Grain Size and Interface Modification via Cesium Carbonate Post-Treatment for Efficient SnO ₂ -Based Planar Perovskite Solar Cells. ACS Applied Energy Materials, 2021, 4, 7002-7011.	2.5	32
97	Facile crystallization control of LaF3/LaPO4:Ce, Tb nanocrystals in a microfluidic reactor using microwave irradiation. Journal of Materials Chemistry, 2010, 20, 1766.	6.7	31
98	White light emission from Mn-doped ZnSe d-dots synthesized continuously in microfluidic reactors. Journal of Materials Chemistry, 2011, 21, 17972.	6.7	31
99	Hydrophobic SiO ₂ Electret Enhances the Performance of Poly(vinylidene fluoride) Nanofiber-Based Triboelectric Nanogenerator. Journal of Physical Chemistry C, 2016, 120, 26600-26608.	1.5	31
100	Largeâ€Grained Perovskite Films Enabled by Oneâ€Step Meniscusâ€Assisted Solution Printing of Crossâ€Aligned Conductive Nanowires for Biodegradable Flexible Solar Cells. Advanced Energy Materials, 2020, 10, 2001185.	10.2	31
101	Flexible 3D Porous MoS ₂ /CNTs Architectures with <i>ZT</i> of 0.17 at Room Temperature for Wearable Thermoelectric Applications. Advanced Functional Materials, 2020, 30, 2002508.	7.8	31
102	Metal–Organic Frameworkâ€Derived Nickel/Cobaltâ€Based Nanohybrids for Sensing Nonâ€Enzymatic Glucose. ChemElectroChem, 2020, 7, 4446-4452.	1.7	30
103	Liquid-liquid interface assisted synthesis of SnO2 nanorods with tunable length for enhanced performance in dye-sensitized solar cells. Electrochimica Acta, 2017, 227, 49-60.	2.6	28
104	Enhanced immunofluorescence detection of a protein marker using a PAA modified ZnO nanorod array-based microfluidic device. Nanoscale, 2018, 10, 17663-17670.	2.8	28
105	Molar ratio of In to urea directed formation of In2O3 hierarchical structures: cubes and nanorod-flowers. CrystEngComm, 2011, 13, 2557.	1.3	27
106	Fabrication of magnetic field induced structural colored films with tunable colors and its application on security materials. Journal of Colloid and Interface Science, 2017, 485, 18-24.	5.0	27
107	Skeleton-Structure WS2@CNT Thin-Film Hybrid Electrodes for High-Performance Quasi-Solid-State Flexible Supercapacitors. Frontiers in Chemistry, 2020, 8, 442.	1.8	27
108	One-pot Hydrothermal Synthesis of N-Doped Carbon Quantum Dots Using the Waste of Shrimp for Hydrogen Evolution from Formic Acid. Chemistry Letters, 2015, 44, 241-243.	0.7	26

#	Article	IF	CITATIONS
109	Facile fabrication of magnetically responsive PDMS fiber for camouflage. Journal of Colloid and Interface Science, 2016, 483, 11-16.	5.0	26
110	Calligraphy-inspired brush written foldable supercapacitors. Nano Energy, 2017, 38, 428-437.	8.2	26
111	A kirigami-inspired island-chain design for wearable moistureproof perovskite solar cells with high stretchability and performance stability. Nanoscale, 2020, 12, 3646-3656.	2.8	26
112	Interfacial Modification via a 1,4-Butanediamine-Based 2D Capping Layer for Perovskite Solar Cells with Enhanced Stability and Efficiency. ACS Applied Materials & amp; Interfaces, 2022, 14, 22879-22888.	4.0	26
113	Anatase TiO2 nanorod arrays as high-performance electron transport layers for perovskite solar cells. Journal of Alloys and Compounds, 2020, 849, 156629.	2.8	25
114	Graphene-carbon nanotube papers for energy conversion and storage under sunlight and heat. Carbon, 2015, 95, 150-156.	5.4	24
115	Microfluidic spinning of editable polychromatic fibers. Journal of Colloid and Interface Science, 2020, 558, 115-122.	5.0	24
116	A portable ascorbic acid in sweat analysis system based on highly crystalline conductive nickel-based metal-organic framework (Ni-MOF). Journal of Colloid and Interface Science, 2022, 616, 326-337.	5.0	24
117	Antisolvent-Derived Intermediate Phases for Low-Temperature Flexible Perovskite Solar Cells. ACS Applied Energy Materials, 2018, 1, 6477-6486.	2.5	23
118	Composite Solid Electrolytes: Facilitating Interfacial Stability Via Bilayer Heterostructure Solid Electrolyte Toward Highâ€energy, Safe and Adaptable Lithium Batteries (Adv. Energy Mater. 31/2020). Advanced Energy Materials, 2020, 10, 2070131.	10.2	23
119	Highly efficient flexible perovskite solar cells made via ultrasonic vibration assisted room temperature cold sintering. Chemical Engineering Journal, 2020, 394, 124887.	6.6	23
120	Ultra-stretchable, self-adhesive, transparent, and ionic conductive organohydrogel for flexible sensor. APL Materials, 2021, 9, .	2.2	23
121	Solvent vapor annealing of oriented PbI2 films for improved crystallization of perovskite films in the air. Solar Energy Materials and Solar Cells, 2017, 166, 167-175.	3.0	22
122	NiCo–NiCoO2/carbon hollow nanocages for non-enzyme glucose detection. Electrochimica Acta, 2021, 381, 138259.	2.6	22
123	Fabrication and magnetic property analysis of monodisperse manganese–zinc ferrite nanospheres. Journal of Magnetism and Magnetic Materials, 2009, 321, 3203-3206.	1.0	21
124	Silver Orthophosphate Immobilized on Flaky Layered Double Hydroxides as the Visible-Light-Driven Photocatalysts. International Journal of Photoenergy, 2012, 2012, 1-6.	1.4	21
125	Surface modification of quartz fibres for dental composites through a sol-gel process. Materials Science and Engineering C, 2017, 74, 21-26.	3.8	21
126	Peptization–Hydrothermal Method as a Surfactantâ€Free Process toward Nanorodâ€Like Anatase TiO ₂ Nanocrystals. European Journal of Inorganic Chemistry, 2009, 2009, 4078-4084.	1.0	20

#	Article	IF	CITATIONS
127	Controllable construction of micro/nanostructured NiO arrays in confined microchannels via microfluidic chemical fabrication for highly efficient and specific absorption of abundant proteins. Journal of Materials Chemistry B, 2015, 3, 4272-4281.	2.9	19
128	Biocompatible and colloidally stabilized mPEG-PE/calcium phosphate hybrid nanoparticles loaded with siRNAs targeting tumors. Oncotarget, 2016, 7, 2855-2866.	0.8	19
129	A strong and flexible electronic vessel for real-time monitoring of temperature, motions and flow. Nanoscale, 2017, 9, 17821-17828.	2.8	19
130	Solution-processed p-type nanocrystalline CoO films for inverted mixed perovskite solar cells. Journal of Colloid and Interface Science, 2020, 573, 78-86.	5.0	19
131	Integrated Ionicâ€Additive Assisted Wetâ€Spinning of Highly Conductive and Stretchable PEDOT:PSS Fiber for Fibrous Organic Electrochemical Transistors. Advanced Electronic Materials, 2021, 7, 2100231.	2.6	19
132	Solvent-controlled formation and photoelectrochemical sensing properties of 3-dimensional TiO2 nanostructures. CrystEngComm, 2011, 13, 6258.	1.3	18
133	A flexible metallic actuator using reduced graphene oxide as a multifunctional component. Nanoscale, 2017, 9, 12963-12968.	2.8	18
134	ZnS–CdS–TaON nanocomposites with enhanced stability and photocatalytic hydrogen evolution activity. Journal of Sol-Gel Science and Technology, 2019, 91, 82-91.	1.1	18
135	High Volumetric Energy Density Asymmetric Fibrous Supercapacitors with Coaxial Structure Based on Graphene/MnO ₂ Hybrid Fibers. ChemElectroChem, 2020, 7, 4641-4648.	1.7	18
136	Preparation of Core/Shell Structured Rutile/Anatase Photocatalyst via Vapor Phase Hydrolysis and its Photocatalytic Degradation of Phenol and Methylene Blue. Journal of the American Ceramic Society, 2012, 95, 1927-1932.	1.9	17
137	Stretchable electrothermochromic fibers based on hierarchical porous structures with electrically conductive dual-pathways. Science China Materials, 2020, 63, 2582-2589.	3.5	17
138	Hierarchical Porous, Selfâ€Supporting La―and Fâ€Codoped TiO ₂ with High Durability for Continuousâ€Flow Visible Light Photocatalysis. Journal of the American Ceramic Society, 2010, 93, 1252-1255.	1.9	16
139	Mechanical design of brush coating technology for the alignment of one-dimension nanomaterials. Journal of Colloid and Interface Science, 2021, 583, 188-195.	5.0	15
140	Core-shell structured SiO2@ZrO2@SiO2 filler for radiopacity and ultra-low shrinkage dental composite resins. Journal of the Mechanical Behavior of Biomedical Materials, 2021, 121, 104593.	1.5	15
141	Electrochemical Actuators with Multicolor Changes and Multidirectional Actuation. Small, 2022, 18, e2107778.	5.2	15
142	Rapid formation of superelastic 3D reduced graphene oxide networks with simultaneous removal of HI utilizing NIR irradiation. Journal of Materials Chemistry A, 2015, 3, 9882-9889.	5.2	14
143	Highly Aligned Molybdenum Trioxide Nanobelts for Flexible Thin-Film Transistors and Supercapacitors: Macroscopic Assembly and Anisotropic Electrical Properties. ACS Applied Nano Materials, 2019, 2, 1466-1471.	2.4	14
144	Flexible photodetector based on cotton coated with reduced graphene oxide and sulfur and nitrogen co-doped graphene quantum dots. Journal of Materials Science, 2019, 54, 3242-3251.	1.7	14

#	Article	IF	CITATIONS
145	Scalable fluid-spinning nanowire-based inorganic semiconductor yarns for electrochromic actuators. Materials Horizons, 2021, 8, 1711-1721.	6.4	14
146	Laser irradiated self-supporting and flexible 3-dimentional graphene-based film electrode with promising electrochemical properties. RSC Advances, 2015, 5, 47074-47079.	1.7	13
147	Solvatochromic structural color fabrics with favorable wearability properties. Journal of Materials Chemistry C, 2019, 7, 4855-4862.	2.7	13
148	Independent dual-responsive Janus chromic fibers. Science China Materials, 2021, 64, 1770-1779.	3.5	13
149	Electrodeposited ternary AgCuO2 nanocrystalline films as hole transport layers for inverted perovskite solar cells. Journal of Alloys and Compounds, 2022, 890, 161879.	2.8	13
150	Multifunctional Mechanical Sensing Electronic Device Based on Triboelectric Anisotropic Crumpled Nanofibrous Mats. ACS Applied Materials & Interfaces, 2021, 13, 55481-55488.	4.0	13
151	Highly integrated fiber-shaped thermoelectric generators with radially heterogeneous interlayers. Nano Energy, 2022, 95, 107055.	8.2	13
152	ZnO/Mg–Al layered double hydroxides as strongly adsorptive photocatalysts. Research on Chemical Intermediates, 2009, 35, 685-692.	1.3	12
153	Fabrication of Hollow Tetrapodâ€Like <scp> <scp>TiN</scp> </scp> Nanostructures and Its Electrochemical Property. Journal of the American Ceramic Society, 2012, 95, 2478-2480.	1.9	12
154	Controllable construction of Titanium dioxide-Zirconium dioxide@Zinc hydroxyfluoride networks in micro-capillaries for bio-analysis. Journal of Colloid and Interface Science, 2015, 446, 290-297.	5.0	12
155	Flow Effects on the Controlled Growth of Nanostructured Networks at Microcapillary Walls for Applications in Continuous Flow Reactions. ACS Applied Materials & Interfaces, 2015, 7, 21580-21588.	4.0	12
156	Three-dimensional ordered titanium dioxide-zirconium dioxide film-based microfluidic device for efficient on-chip phosphopeptide enrichment. Journal of Colloid and Interface Science, 2016, 478, 227-235.	5.0	12
157	Visibly vapor-responsive structurally colored carbon fibers prepared by an electrophoretic deposition method. RSC Advances, 2016, 6, 16319-16322.	1.7	12
158	Light-driven artificial muscles based on electrospun microfiber yarns. Science China Technological Sciences, 2019, 62, 965-970.	2.0	12
159	Highly efficient walking perovskite solar cells based on thermomechanical polymer films. Journal of Materials Chemistry A, 2019, 7, 26154-26161.	5.2	12
160	Controlled preparation of β-Bi2O3/Mg–Al mixed metal oxides composites with enhanced visible light photocatalytic performance. Research on Chemical Intermediates, 2020, 46, 5009-5021.	1.3	12
161	Ultra-stable ionic-liquid-based electrochromism enabled by metal-organic frameworks. Cell Reports Physical Science, 2022, 3, 100866.	2.8	12
162	Formation of the modified ultrafine anatase TiO2 nanoparticles using the nanofiber as a microsized reactor. CrystEngComm, 2013, 15, 1607.	1.3	11

#	Article	IF	CITATIONS
163	Enhancement in photoelectric performance of flexible perovskite solar cells by thermal nanoimprint pillar-like nanostructures. Materials Letters, 2019, 248, 16-19.	1.3	11
164	High power factor n-type Ag ₂ Se/SWCNTs hybrid film for flexible thermoelectric generator. Journal Physics D: Applied Physics, 2021, 54, 434004.	1.3	11
165	Controlling the transformation of intermediate phase under near-room temperature for improving the performance of perovskite solar cells. Solar Energy, 2019, 186, 225-232.	2.9	10
166	Enhanced fluorescence and heat dissipation of calcium titanate red phosphor based on silver coating. Journal of Colloid and Interface Science, 2015, 459, 44-52.	5.0	9
167	Anion effect on properties of Zn-doped CH3NH3PbI3 based perovskite solar cells. Solar Energy Materials and Solar Cells, 2021, 233, 111400.	3.0	9
168	Capillary force driven printing of asymmetric Na-ion micro-supercapacitors. Journal of Materials Chemistry A, 2020, 8, 22083-22089.	5.2	8
169	An electrically controllable all-solid-state Au@graphene oxide actuator. Chemical Communications, 2016, 52, 5816-5819.	2.2	7
170	Facile synthesis of 3D hierarchical micro-/nanostructures in capillaries for efficient capture of circulating tumor cells. Journal of Colloid and Interface Science, 2020, 575, 108-118.	5.0	7
171	Enhanced Visible Lightâ€Driven Photocatalytic Performance of Laâ€Doped TiO _{2â^'<i>x</i>} F _{<i>x</i>} . Journal of the American Ceramic Society, 2010, 93, 25-27.	1.9	6
172	Synthesis of Mesoporous (Ga _{1â^²} <i>_x</i> Zn <i>_x</i>)(N _{1â^²} <i>_x</i> O <i> Using Layered Double Hydroxides as Precursors for Enhanced Visibleâ€Light Driven H₂ Production. Chinese Journal of Chemistry, 2017, 35, 196-202.</i>	sub>x2.6	up\$)
173	Additionalâ€Heatingâ€Enhanced Largeâ€Scale Metallic Molybdenum Disulfide Nanosheet Exfoliation for Freeâ€Standing Films and Flexible Highâ€Performance Supercapacitors. ChemNanoMat, 2020, 6, 267-273.	1.5	4
174	Atomic layer deposition SiO2 films over dental ZrO2 towards strong adhesive to resin. Journal of the Mechanical Behavior of Biomedical Materials, 2021, 114, 104197.	1.5	4
175	Dielectrophoretic Assembly of Carbon Nanotube Chains in Aqueous Solution. Advanced Fiber Materials, 2021, 3, 312-320.	7.9	4
176	Continuous preparation of dual-responsive sensing fibers for smart textiles. Journal of Colloid and Interface Science, 2021, 597, 215-222.	5.0	4
177	Graphene-based implantable neural electrodes for insect flight control. Journal of Materials Chemistry B, 2022, 10, 4632-4639.	2.9	4
178	Eu doped Si-oxynitride fluorescent nanofibrous inorganic membranes with high flexibility. RSC Advances, 2015, 5, 101287-101292.	1.7	3
179	Mesoporous Pt/TiO2-xNx nanoparticles with less than 10 nm and high specific surface area as visible light hydrogen evolution photocatalysts. Journal of Sol-Gel Science and Technology, 2018, 87, 230-239.	1.1	3
180	Highly fluorinated polyimide gate dielectric for fully transparent aqueous precursor derived In–Zn oxide thin-film transistors. Journal of Materials Science, 2020, 55, 15919-15929.	1.7	3

#	Article	IF	CITATIONS
181	Synergistic Effect of <i>N</i> , <i>N</i> -Dimethylformamide and Hydrochloric Acid on the Growth of MAPbl ₃ Perovskite Films for Solar Cells. ACS Omega, 2020, 5, 32295-32304.	1.6	3
182	Dual Covalent Cross-Linking Networks in Polynorbornene: Comparison of Shape Memory Performance. Materials, 2021, 14, 3249.	1.3	3
183	Redox-Active Ni(II) Nodes Induced Electrochromism in a Two-Dimensional Conductive Metal–Organic Framework. ACS Applied Electronic Materials, 2022, 4, 2915-2922.	2.0	3
184	A self-healing, Na+ sensitive and neuron-compatible fiber. Chemical Engineering Journal, 2020, 386, 124018.	6.6	2
185	FOAMING AND MOISTURE CROSSLINKING OF VINYL TRIETHOXY SILANE GRAFTED ETHYLENE–PROPYLENE–DIENE TERPOLYMER. Rubber Chemistry and Technology, 2022, 95, 479-491.	0.6	2
186	Fabrication of LiMnPO4-MWCNT cathode material via vapor phase hydrolysis and its electrochemical properties. Ionics, 2015, 21, 651-656.	1.2	1